PERGAMON

Phytochemistry 52 (1999) 281–289

PHYTOCHEMISTRY

Structures of 5-alkylresorcinol-related analogues in rye

Yoshikatsu Suzuki*, Yasuaki Esumi, Isamu Yamaguchi

The Institute of Physical and Chemical Research (RIKEN), Hirosawa 2-1, Wako-shi, Saitama, 351-0198, Japan

Received 23 September 1998; received in revised form 29 January 1999

Abstract

A series of 5-(2′-oxo)alkylresorcinols, 5-(2′- and 4′-hydroxy)alkylresorcinols, and 5,5′-(alkadiyl)diresorcinols were isolated from rye, each as a mixture of homologues. The identification of these alkylresorcinol-related analogues was achieved by analyses of the ^{1}H-NMR and MS spectra. From the identity of the analogues found, a possible biosynthetic pathway to the 2′-oxoalkylresorcinols is proposed, based on a correlation of the carbon-chain lengths between the alkylresorcinols and 2′-oxoalkylresorcinols.

Keywords: Secale sereale L; Gramineae; Oxoalkylresorcinol; Hydroxyalkylresorcinol; Alkadiyldiresorcinol

1. Introduction

Recently, Suzuki, Esumi, Hyakutake, Kono and Sakurai (1996) and Bouillant, Jacoud, Zanella, Favre-Bonvin and Bally (1994) reported the identification of 5-alkylresorcinols (ARs) from rice as antifungal agents accumulated specifically in etiolated seedlings. In our subsequent work (Suzuki et al., 1998), 5-(2′-oxo)alkylresorcinols (2′-OARs) were identified as rice AR-related analogues, and a hypothetical biosynthetic pathway of 2′-OARs was proposed based on a correlation between the double-bond positions of ARs and 2′-OARs. Similar ARs also exist in rye and wheat during the early to mature stages of kernel development and are believed to act partly as antifungal agents (Verdeal & Lorenz, 1977). We have determined the carbon-chain structures of all the known rye and wheat ARs (Suzuki, Esumi, Uramoto, Kono & Sakurai, 1997). These studies have led us to recognize the following structural differences between rice and rye ARs: (a) the alkyl chain lengths in rye are longer than those in rice, (b) each homologue with alkenyl chains in rye is a double-bond position isomer, unlike those in rice, and (c) the double-bonds are in fixed positions relative to the methyl groups in the ARs of rye, while they are fixed relative to the 5-carbons of the resorcinol moieties in the ARs of rice. In addition, the accumulation stages are quite different between rye and rice ARs (Suzuki, Saitoh, Hyakutake, Kono & Sakurai, 1996). To determine that these structural differences between rye and rice ARs are derived from differences existing in their ARs biosynthetic pathways, identification of AR-related analogues in rye was undertaken.

In this report, the isolation and identification of four kinds of AR-related analogues, **1** (2′-OAR), **2** [5-(4′-hydroxy)alkylresorcinol (4′-HAR)], **3** [5-(2′-hydroxy)alkylresorcinol (2′-HAR)], and **4** [5,5′-(alkadiyl)diresorcinol (ADR)] in rye are described. The possible biosynthetic pathways of the 2′-OARs is hypothesized, based on comparisons of the alkyl-chain lengths between the ARs and 2′-OARs.

2. Results and discussion

The acetone extract from rye whole flour (2.0 kg) was fractionated using a silica-gel column. Four AR-related analogues, **1**–**4**, were located by a color reaction on TLC and by ^{1}H-NMR spectra. Silica-gel col-

* Corresponding author. Fax: +81-48-462-4676.
E-mail address: yoshi@postman.riken.go.jp (Y. Suzuki)

0031-9422/99/$ - see front matter
PII: S0031-9422(99)00196-X

Table 1
^{1}H-NMR spectral data for the AR-related analogues (400 MHz)

Carbon no.	**1**(2′-OARs), $CDCl_3$	**2**(4′-HARs), $CDCl_3+CD_3OD$	**3**(2′-HARs),$CDCl_3+CD_3OD$	**4**(ADRs), d_6-acetone
1′ (1″)	3.55 *s* (2H)	2.39 *m* (2H)	2.40 *dd* (1H, *J* = 13.4, 8.9) 2.63 *dd* (1H, *J* = 13.4, 3.9)	2.43 *m* (4H, *J* = 7.6)
2′ (2″)		1.31–1.7 *m* (4H)	3.70 *m* (1H)	1.55 *m* (4H)
3′	2.46 *t* (2H, *J* = 7.3)			
4′	1.53 *m* (2H)	3.48 *m* (1H)		
—CH_2—	1.23 *m* (ca 29H)	1.16 *m* (ca 34H)	1.20 *m* (ca 26H)	1.27 *m* (ca 27H)
—CH_3	0.86 *t* (3H, *J* = 6.6)	0.79 *t* (3H, *J* = 6.8)	0.82 *t* (3H, *J* = 6.7)	
2 (2′)	6.22 *s* (1H)	6.05 *t* (1H, *J* = 2.0)	6.13 *t* (1H, *J* = 2.0)	6.16 *t* (2H, *J* = 2.0)
4,6 (4′,6′)	6.22 *s* (2H)	6.11 *d* (2H, *J* = 2.0)	6.15 *d* (2H, *J* = 2.0)	6.17 *d* (4H, *J* = 2.0)
1,3 (1′,3,)—OH	6.08 *br,s* (2H)			7.99 *s* (4H)
=CH—	5.33 *m* (ca 0.8H)	5.26 *m* (ca 0.6H)	5.29 *m* (ca 0.29H)	5.35 *m* (ca 0.32H)
=$CHCH_2$—	1.99 *m* (ca 1.4H)	1.93 *m* (ca 1H)	1.97 *m* (ca 0.62H)	–[a]
=$CHCH_2CH$=	2.75 *m* (ca 0.11H)	2.70 *m* (ca 0.12H)	–[a]	–[a]

[a] Overlapping with the solvent peaks.

umn chromatograph of each fraction containing the AR-related analogues, followed by a preparative TLC, yielded **1** (40.8 mg), **2** (2 mg), **3** (2 mg), or **4** (1 mg), as single spots on TLC.

2.1. Gross structures of the AR-related analogues

The ^{1}H-NMR and MS analyses of the isolated AR-related analogues, as described below, provided evidence on their basic skeletal structures and enabled the determination of alkyl-chain length and the degree of double-bond unsaturation. Table 1 summarizes their ^{1}H-NMR spectral data. Fig. 1 illustrates the determined skeletal structures.

Analogue **1** was identified to be a 5-(2′-oxo)alkylresorcinol (2′-OAR), owing to its similarities in the ^{1}H-NMR spectral data and *Rf* values on TLC, with the known rice 2′-OARs (Suzuki et al., 1998). The $[M-H]^-$ ion peaks in the FAB/MS spectrum indicated that **1** is a mixture of C_{17} to C_{27} homologues.

Analogue **2** exhibited aromatic proton signals at δ 6.05 and 6.11 ppm in the ^{1}H-NMR spectrum, characteristic of a 5-alkyl-substituted resorcinol moiety, together with the signals at δ 2.39, 3.48, 0.79, and 1.16 ppm assigned as a benzylic methylene, methine adjacent to a hydroxyl group, methyl, and methylenes, respectively. The molecular formulae which were calculated from the $[M-H]^-$ ion peaks of the high-resolution FAB/MS spectrum confirmed the presence of a hydroxyl group. Thus, **2** was identified to be a hydroxyalkyl-substituted resorcinol. The position of the hydroxyl group was subsequently determined to be on the 4′-carbon using the high-energy collision-activated dissociation (CAD) spectra for each component. For example, the CAD spectrum from the $[M-H]^-$ ion (*m*/*z* 447) of $C_{23:0}$ homologue, is shown in Fig. 2. The CAD spectrum of an alkyl carbon-chain with a hydroxyl group is expected to show a window of 30 amu formed by the two fragment ion peaks cleaved on either side of the hydroxyl group, due to charge-remote fragmentations (Adams, 1990). Such a window was found at *m*/*z* 179/149. The position of the window shows that the hydroxyl group is located at the 4′-carbon. The CAD spectrum from the $[M+Li]^+$ ion (*m*/*z* 455) of the $C_{23:0}$ homologue confirmed this result as the window was observed at the corresponding fragment ion position, *m*/*z* 187/157 (spectrum not shown). In a similar manner, the positions of the hydroxyl groups for other homologues of **2** were also shown to be at the 4′-carbons. Thus, analogue **2** was determined to be a 5-(4′-hydroxy)alkylresorcinol (4′-HAR).

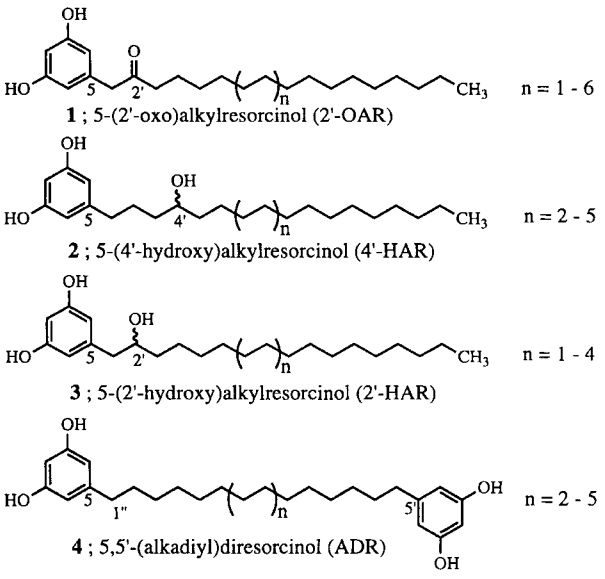

Fig. 1. Skeletal structures of AR-related analogues in rye.

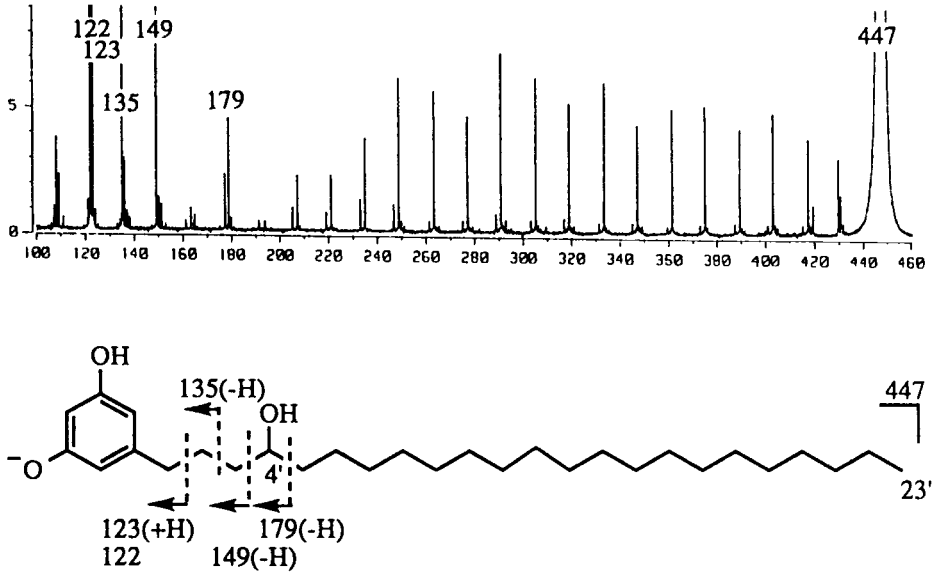

Fig. 2. CAD spectrum of $C_{23:0}$ homologue.

Analogue **3** also had a 5-alkyl-substituted resorcinol moiety detected by the presence of characteristic aromatic proton signals at δ 6.13 and 6.15 ppm in the ^{1}H-NMR spectrum. In addition, the two doublet of doublet signals at δ 2.40 and 2.63 ppm, assigned as the benzylic methylene, were coupled with the multiplet signal at δ 3.70 ppm, assigned as a methine adjacent to a hydroxyl group. This coupling indicated that the hydroxyl group is on the 2′-carbon of the alkyl group. Thus, **3** was identified to be a 5-(2′-hydroxy)alkylresorcinol (2′-HAR) (Su, Reusch & Sadoff, 1981).

Analogue **4** exhibited aromatic proton signals at δ 6.16 and 6.17 ppm, characteristic of a 5-alkyl-substituted resorcinol moiety, and a benzylic methylene proton signal at δ 2.43 ppm in the ^{1}H-NMR spectrum. The absence of a terminal-methyl proton signal implies that the methyl group is substituted by another group. The molecular formulae based on the high-resolution FAB/MS spectrum indicated the presence of a resorcinol moiety as the substituent. Thus, **4** was identified to be a 5,5′-(alkadiyl)diresorcinol (ADR) (Cirigottis et al., 1974; Scannel, Barr, Murty, Reddy & Hecht, 1988).

Similar to rye ARs (Verdeal & Lorenz, 1977) these four AR-related analogues were co-isolated with the corresponding alkenyl (monoene system) and alkadienyl (a homoconjugated-diene system) homologue series as minor constituents. The presence of vinyl and allylic proton signals in the ^{1}H-NMR spectra confirmed the presence of these double-bonds in the alkyl carbon-chains. The approximate composition estimated from the relative intensities of the $[M-H]^-$ ion peaks in the FAB/MS spectra were 69–75% for the saturated alkyl, 21–29% for the alkenyl, and 3–7% for the alkadienyl series. Of the four AR-related analogues, the 2′-OARs were separated into the three homologue series, those with saturated carbon-chains, monoenes, and dienes in order to obtain better CAD spectra. These separations were achieved by the use of a preparative TLC on silica gel impregnated with silver nitrate, as for rye ARs (Suzuki et al., 1997).

2.2. Structures of the alkyl groups in the AR-related analogues

The positions of the double-bonds for all AR-related analogues were determined using CAD spectra for each component, using the same method as that described for rice and rye ARs and rice 2′-OARs (Suzuki et al., 1997, 1998).

Fig. 3 illustrates the CAD spectra for the three alkyl-type of the 2′-OARs. The spectrum (i) of 2′-$OAR_{23:0}$ with a saturated carbon-chain gave rise to a sequence of odd-mass series fragments that was regularly spaced by 14 amu, after an initial loss of methane (16 amu). Such fragment patterns, due to charge-remote fragmentations, are characteristic of a linear carbon-chain structure. Also, in other 2′-OARs with saturated carbon-chains, similar fragment patterns were observed. Thus, all of these saturated carbon-chains were determined to be linear.

The positions of double-bonds in the 2′-OARs were determined using the location of 54 amu windows, characteristic of monoenes, or a pair of 40 and 54 amu windows, characteristic of homoconjugated-dienes that arise from abundant fragment ion peaks produced by allylic cleavage and less-abundant peaks produced by vinylic cleavage. However, the CAD spectra of the 2′-OARs with monoenes did not reveal the typical 54 amu window, and analysis is extremely complicated,

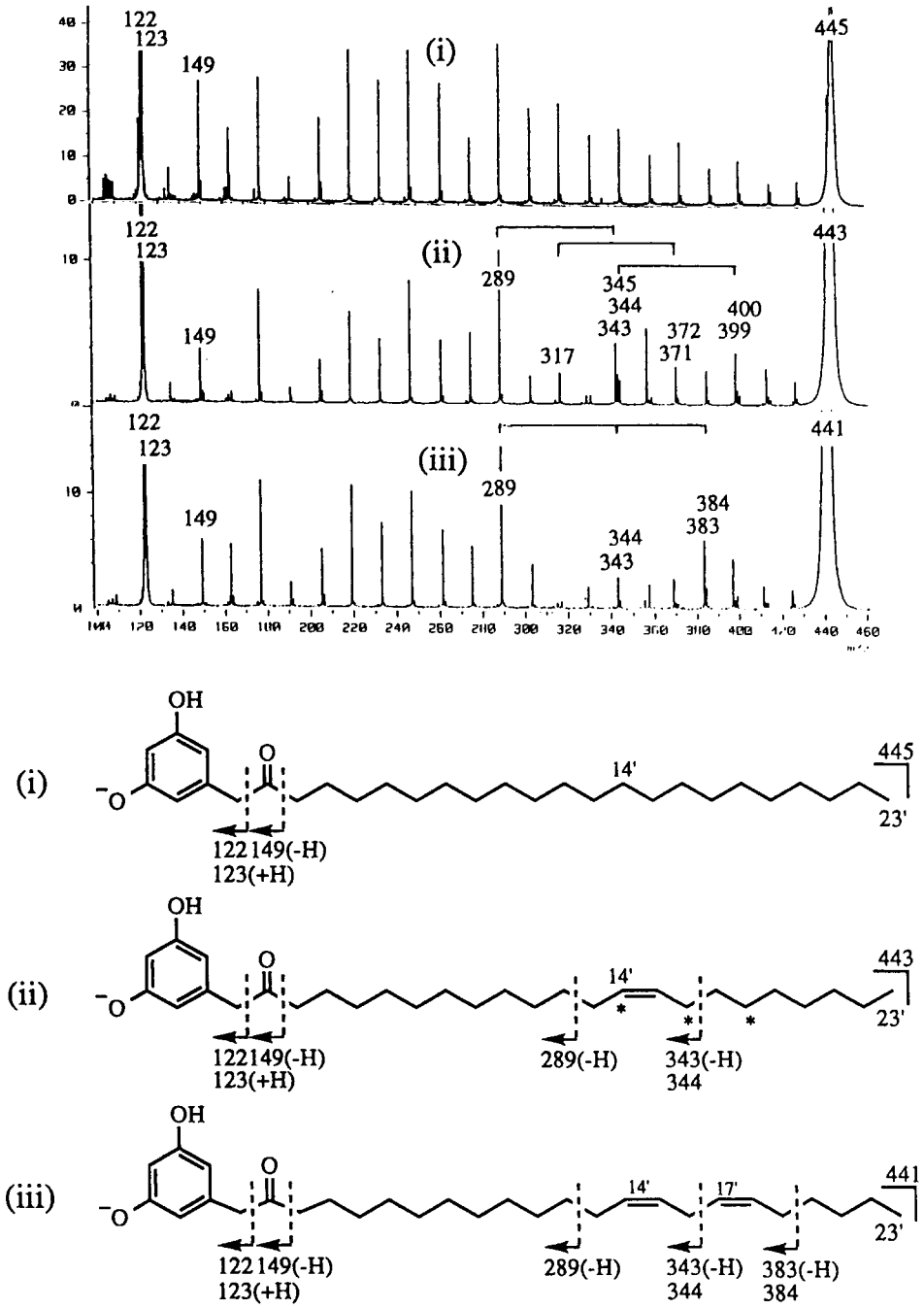

Fig. 3. CAD spectra of 2′-OAR_{23}.

similar to that of the CAD spectra of rye and wheat ARs that consist of double-bond positional isomers (Suzuki et al., 1997). This indicates that the 2′-OARs with monoenes are also double-bond positional isomers. Therefore, the double-bond positions of the analogues with alkenyl substituents were determined by the same method as used for rye ARs (Suzuki et al., 1997), with the guidance of the fragment ion peaks of an even mass series due to radical cleavage at the allylic position of the methyl terminus, together with the window of 54 amu. For example, in the spectrum (ii) of 2′-$OAR_{23:1}$, three sets of 54 amu windows were found at *m/z* 343/289, 371/317, and 399/345, together with the corresponding radical ion peaks at m/z 344, 372, and 400. This led to the deduction that the double-bonds are located at the 14′, 16′, and 18′-carbons, respectively.

All 2′-OARs with homoconjugated-dienes showed the typical 40 and 54 amu window pairs in the CAD spectra. For example, in the spectrum (iii) of 2′-

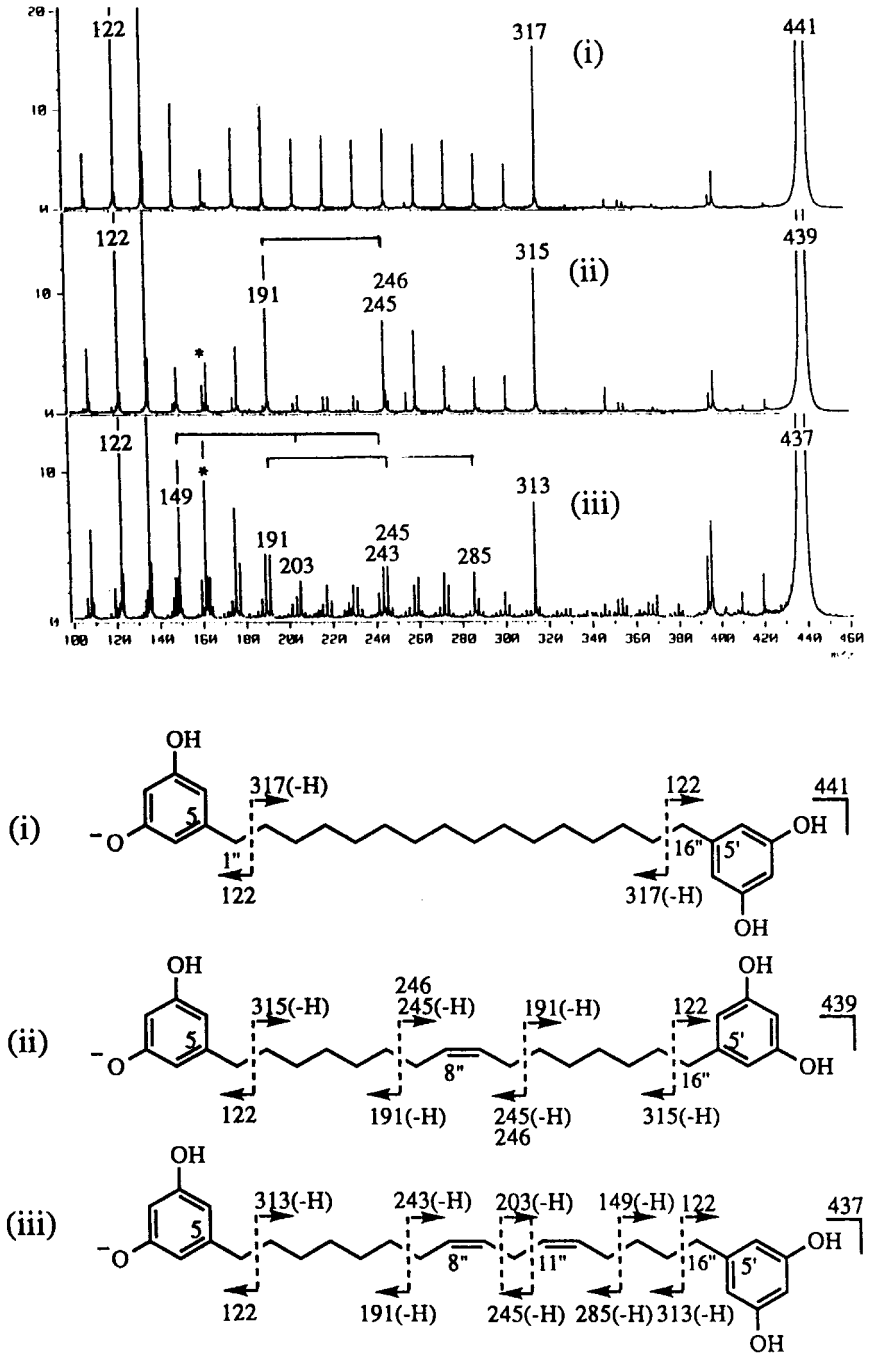

Fig. 4. CAD spectra of ADR_{16}

$OAR_{23:2}$, the windows were found at m/z 383/343 and 343/289, together with the radical ion fragments at m/z 384 and 344, showing that the double-bonds are located at the 14′, 17′-carbons.

Fig. 4 illustrates the CAD spectra for the three alkyl-type ADRs. The spectra of ADRs with saturated carbon-chains gave fragment patterns characteristic of a linear carbon-chain structure, as shown in the spectrum (i) of $ADR_{16:0}$: a sequence of odd-mass series that was regularly spaced by 14 amu after an initial loss of 3-hydroxytropone or its equivalents (122 amu). Thus, all of these saturated carbon-chains of ADRs were determined to be linear.

The position of double-bonds in ADRs was also determined using the location of the windows, characteristic of monoenes and of homoconjugated-dienes. The spectrum (ii) of ADR16:1 was shown as a typical example, and provided the typical 54 amu window only at m/z 245/191, together with the radical ion peak at m/z 246. This is unambiguous evidence of the

Table 2
Structures of the AR-related analogues in rye

Alkyl-chain length	C_{17}	C_{19}	C_{21}	C_{23}	C_{25}	C_{27}
(2′-OARs)						
alkyl	#[a]	#	#	#	#	#
alkenyl	ND[b]	10′/12′/14′	12′/14′/16′	14′/16′/18′	16′/18′/20′	ND
alkadienyl	ND	10′,13′	12′,15′	14′,17′	16′19′	18′,21′
4′-HARs						
alkyl		#	#	#	#	
alkenyl		ND	12′/14′16′	16′/18′	16′/18′/20′	
alkadienyl		ND	12′,15′	14′,17′	ND	
2′-HARs						
alkyl	#	#	#	#		
alkenyl	ND	10′/12′/14′	12′/14′/16′	ND		
alkadienyl	ND	ND	ND	ND		

Alkyl-chain length	C_{16}	C_{18}	C_{20}	C_{22}
ADRs				
alkyl	#	#	#	#
alkenyl	8″	10″	ND	ND
alkadienyl	8″,11″	10″,13″	ND	ND

[a] ## = Linear carbon-chains.
[b] ND = Not determined.

double-bond being located at the 8″-carbon. However, when the double-bond exists at asymmetric positions, two series of windows should be observed. The spectrum of $ADR_{18:1}$ is such a case, and provided two sets of 54 amu windows at *m/z* 273/219 and 245/191, together with the radical ion peaks at *m/z* 274 and 246 (spectrum not shown). This showed that the double-bond is located at the 10″-carbon.

The ADR with homoconjugated-dienes also did not show the typical 40 and 54 amu window pair in the CAD spectra. For example, the spectum (iii) of $ADR_{16:2}$ provided two window pairs at *m/z* 285/245 and 245/191 and at 243/203 and 203/149. If the double-bonds were located at asymmetric positions, these window positions show that the double-bonds would be located at the 8″, 11″-carbons. Also, $ADR_{18:2}$ provided two pairs of windows at *m/z* 271/231 and 231/177 and at 285/245 and 245/191 (spectrum not shown), showing that the double-bonds are located at the 10″, 13″-carbons.

The structures of the alkyl groups in the 2′-HARs and 4′-HARs were also determined using the same method as that described for the 2′-OARs. Table 2 summarizes the carbon-chain lengths and double-bond positions determined for the AR-related analogues in rye. The geometry of the double-bonds and the absolute configurations of the hydroxyl groups of the 4′- and 2′-HARs were not determined. However, the double-bonds are assumed to be the Z type, based on the biosynthetic correlation of the AR-related analogues with ARs, as described below. To our knowledge, the 2′-OARs (C_{21} to C_{27}), 4′-HARs (C_{19} to C_{25}), 2′-HARs (C_{17} to C_{23}) except 2′-$HAR_{21:0}$ and 2′-$HAR_{23:0}$ (Adams, 1990), and all ADRs (C_{16} to C_{22}) except $ADR_{16:1}$ (Su et al., 1981) had not been identified previously.

Of the AR-related analogues determined, the saturated carbon-chains were all linear. Each homologue with a homoconjugated-diene is composed of single isomer, while each homologue with a monoene is composed of double-bond positional isomers, except the ADRs. In addition, there exists regularity in the double-bond positions among the rye ARs and AR-related analogues, as illustrated in Fig. 5. The double-bonds in the ARs, 2′-OARs, and 4′- and 2′-HARs are located commonly at the ω9, ω7, or ω5 carbons for

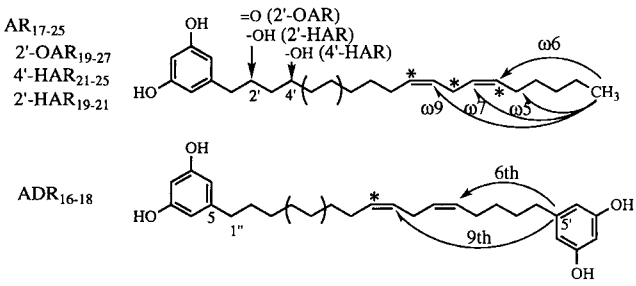

Fig. 5. Positions of double-bonds in AR-related analogues. *Positions of the monoene (ω9, ω7, ω5 and 9th).

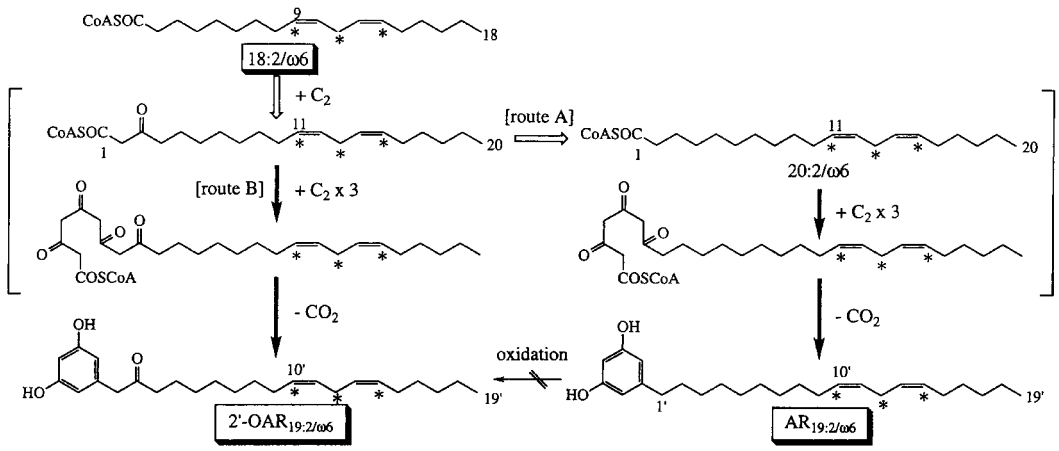

Fig. 6. Possible biosynthetic pathways to 2′-OARs in rye. *Positions of the monoenes (ω9, ω7, and ω5); ⇒ chain-elongation processes; → malonate condensation and/or decarboxylation processes.

the monoenes (*), and at the ω6 carbons for the dienes, regardless of carbon-chain length. Similar regularity was also found for ADRs; the double-bonds are located at the 6th-carbon for the dienes and at the 9th-carbon for the monoenes, from the 5′-aromatic carbons. The regularity in double-bond positions of the ARs and 2′-OARs suggests possible biosynthetic pathways for the 2′-OARs. Fig. 6 illustrates the possible biosynthetic pathways to the 2′-OARs. Two possible biosynthetic routes are considered, via an oxidation of the 2′-methylene group (route A) and via a β-oxo-fatty acid derivative (route B) that is an intermediate during the chain-elongation process of fatty acids. The double-bond positions determined gave no information on which route occurs in rye, because there are no differences in the double-bond positions between ARs and 2′-OARs with the same carbon-chain lengths (Fig. 5). However, a comparison of the carbon-chain lengths between ARs and 2′-OARs provided some clues. Composition (%) of both homologues with saturated carbon-chains was estimated from the relative intensities of the $[M-H]^-$ ion peaks in the FAB/MS spectra; 29.7/C_{17}, 33.8/C_{19}, 20.5/C_{21}, 8.7/C_{23}, and 7.2/C_{25}) for the ARs, and 2.0/C_{17}, 24.6/C_{19}, 30.5/C_{21}, 31.5/C_{23}, 9.4/C_{25}, 2.0/C_{27} for the 2′-OARs. The chain lengths of the main homologues are C_{17} to C_{21} for the ARs and C_{19} to C_{23} for the 2′-OARs. That is, the minimum and maximum chain lengths of the 2′-OARs are C_2-unit longer than those of the ARs. In the route A, the main 2′-OARs would be homologues of the C_{17} to C_{21} chains if oxidation at the 2′-methylenes in the ARs occurred regardless of the chain lengths. The rye 2′-OARs are therefore predicted to be formed via a β-oxo-fatty acid derivative of route B as previously predicted for those of rice (Suzuki et al., 1998). Such chain length range shifts have also been detected between the rice ARs and 2′-OARs (unpublished observations). Based on this hypothesis, the reason for the regularity for all the double-bond positions of the 2′-OARs can be speculated as follows. Desaturation of $C_{18:0}$ fatty acid derivative by 9-dehydrogenase or 9- and 12-dehydrogenases produces the corresponding unsaturated derivatives $C_{18:1/\omega9}$ and $C_{18:2/\omega6}$. Subsequent chain-elongations of each unsaturated fatty acid derivative produce the $C_{20:1/\omega9}$ to $C_{26:1/\omega9}$ and $C_{20:2/\omega6}$ to $C_{28:2/\omega6}$ homologues, which form ARs and 2′-OARs with the corresponding monoenes of the ω9 series and dienes of the ω6 series. The ω7 and ω5 series of ARs and 2′-OARs with monoenes are formed from the shorter fatty acid derivatives of $C_{14:0}$ and $C_{16:0}$ in the same reactions as those described for the ω9 series.

3. Experimental

3.1. General

NMR spectra were recorded with TMS as an internal standard. TLC was conducted with precoated plates (0.25 mm thickness) of silica gel F_{254}. As TLC spray reagent, 5% vanillin in conc sulfuric acid solution was used.

3.2. Isolation of AR-related analogues in rye whole flour

Rye whole flour (2.0 kg) was extracted with acetone (5 l). The acetone extract was chromatographed on a silica gel column (ϕ30 mm × 200 mm). Elution with 10–20% EtOAc–CH_2Cl_2 gave the crude fractions of ARs (3.2 g), **1** (249 mg), **2** (62 mg), and a mixture of **3** and **4** (60 mg). The AR-related analogues were detected as red to red-brown spots by the TLC spray reagent. The fraction of **1** was purified using a silica-gel column (ϕ11 mm × 80 mm) with 2% MeOH–$CHCl_3$, followed by a preparative TLC on silica-gel

with 25% EtOAc–CH_2Cl_2, giving 2′-OARs (**1**, 40.8 mg) as a single spot on TLC. 4′-HARs (**2**, 2 mg), 2′-HARs (**3**, 2 mg), and ADRs (**4**, 1 mg) were isolated in a similar manner. The *Rf* values of the AR-related analogues on TLC with 5% MeOH–$CHCl_3$ were 0.57 (2′-OARs), 0.47 (4′- and 2′-HARs), and 0.26 (ADRs).

3.3. 2′-OARs

^{1}H NMR (400 MHz, $CDCl_3$): Table 1; FAB/MS *m/z* $[M-H]^-$ (Rel. int.): 361 (6.3), 385 (3.1), 387 (14.0), 389 (78.1), 413 (7.8), 415 (46.8), 417 (96.8), 441 (10.9), 443 (46.9), 445 (100), 469 (3.1), 571 (10.9), 573 (29.7), 501 (6.3), high-resolution FAB/MS *m/z* $[M-H]^-$: found, 361.2715, calcd. 361.2742 ($C_{23}H_{37}O_3$); found, 387.2923, calcd. 387.2893 ($C_{25}H_{39}O_3$); found, 389.3039, calcd. 389.3056 ($C_{25}H_{41}O_3$); found, 413.3069, calcd. 413.3056 ($C_{27}H_{41}O_3$); found, 415.3224, calcd. 415.3213 ($C_{27}H_{43}O_3$); found, 417.3399, calcd. 417.3369 ($C_{27}H_{45}O_3$); found, 441.3397, calcd. 441.3369 ($C_{29}H_{45}O_3$); found, 443.3552, calcd. 443.3526 ($C_{29}H_{47}O_3$); found, 445.3701, calcd. 445.3681 ($C_{29}H_{49}O_3$); found, 471.3804, calcd. 471.3838 ($C_{31}H_{51}O_3$); found, 473.4026, calcd. 473.3995 ($C_{31}H_{53}O_3$); found, 501.4312, calcd. 501.4307 ($C_{33}H_{57}O_3$).

3.4. Separation of the homologues of 2′-OARs

The native 2′-OAR (30 mg) was charged on silica gel plates (20 cm × 20 cm × 0.25 mm, 6 plates) impregnated with 15% silver nitrate in EtOH–H_2O (1:1). The plates were developed once with 5% MeOH–$CHCl_3$ up to a height of 10 cm and then by a second development to a height of 15 cm. Three bands, *Rf* 0.29–0.32, *Rf* 0.21–0.29, and *Rf* 0.14–0.21, were observed upon visualization by spraying with distilled H_2O. Each of the bands was scraped off and eluted with 10% MeOH–$CHCl_3$, giving the 2′-oxo-alkyl (17.4 mg, powder), 2′-oxo-alkenyl (5.3 mg, oil) and 2′-oxo-alkadienyl resorcinols (1.1 mg, oil).

3.5. 4′-HARs

^{1}H NMR (400 MHz, $CDCl_3 + CD_3OD$): Table 1; FAB/MS *m/z* $[M-H]^-$ (Rel. int.): 391 (15.9), 415 (3.0), 417 (26.8), 419 (100), 443 (3.0), 445 (18.9), 447 (50.0), 471 (2.4), 473 (15.9), 475 (43.9), 501 (7.3), 503 (30.5), high-resolution FAB/MS *m/z* $M-H]^-$: found, 391.3232, calcd. 391.3212 ($C_{25}H_{43}O_3$); found, 415.3233, calcd. 415.3212 ($C_{27}H_{43}O_3$); found, 417.3357, calcd. 417.3368 ($C_{27}H_{45}O_3$); found, 419.3537, calcd. 419.3525 ($C_{27}H_{47}O_3$); found, 443.3553, calcd. 443.3525 ($C_{29}H_{47}O_3$); found, 445.3700, calcd. 445.3681 ($C_{29}H_{49}O_3$); found, 447.3841, calcd. 447.3839 ($C_{29}H_{51}O_3$); found, 471.3830, calcd. 471.3839 ($C_{31}H_{51}O_3$); found, 473.4007, calcd. 473.3995 ($C_{31}H_{53}O_3$); found, 475.4160, calcd. 475.4152 ($C_{31}H_{55}O_3$); found, 501.4307, calcd. 501.4308 ($C_{33}H_{57}O_3$); found, 503.4492, calcd. 503.4464 ($C_{33}H_{59}O_3$).

3.6. 2′-HARs

^{1}H NMR (400 MHz, $CDCl_3 + CD_3OD$): Table 1; FAB/MS *m/z* $[M-H]^-$ (Rel. int.): 363 (14.7), 387 (6.2), 389 (26.4), 391 (100.0), 415 (5.4), 417 (15.8), 419 (44.2), 447 (11.6), high-resolution FAB/MS *m/z* $[M-H]^-$: found, 363.2919, calcd. 363.2899 ($C_{23}H_{39}O_3$); found, 389.3062, calcd. 389.3056 ($C_{25}H_{41}O_3$); found, 391.3233, calcd. 391.3212 ($C_{25}H_{43}O_3$); found, 417.3391, calcd. 417.3369 ($C_{27}H_{45}O_3$); found, 419.3546, calcd. 419.3525 ($C_{27}H_{47}O_3$); found, 447.3830, calcd. 447.3838 ($C_{29}H_{51}O_3$).

3.7. ADRs

^{1}H NMR (400 MHz, d_6-acetone): Table 1; FAB/MS *m/z* $[M-H]^-$ (Rel. int.): 437 (3.1), 439 (32.0), 441 (100.0), 465 (3.1), 467 (13.3), 469 (22.7), 497 (3.1), 525 (0.8), high-resolution FAB/MS *m/z* $[M-H]^-$: found, 437.2714, calcd. 437.2692 ($C_{28}H_{37}O_4$); found, 439.2864, calcd. 439.2848 ($C_{28}H_{39}O_4$); found, 441.3015, calcd. 441.3004 ($C_{28}H_{41}O_4$); found, 465.3023, calcd. 465.3064 ($C_{30}H_{41}O_4$); found, 467.3163, calcd. 467.3161($C_{30}H_{43}O_4$); found, 469.3310, calcd. 469.3318 ($C_{30}H_{45}O_4$); found, 497.3659, calcd. 497.3631 ($C_{32}H_{49}O_4$); found, 525.3929, calcd. 525.3944 ($C_{34}H_{53}O_4$).

3.8. ARs (Suzuki et al., 1997)

FAB/MS *m/z* $[M-H]^-$ (Rel. int.): 343 (10.0), 345 (36.3), 347 (87.8), 371 (15.1), 373 (59.0), 375 (100), 399 (15.1), 401 (40.9), 403 (60.6), 427 (6.0), 429 (20.6), 431 (25.7), 455 (5.4), 457 (16.0), 459 (21.2).

3.9. FAB/MS and CAD spectra

A JMS HX-110/110A tandem mass spectrometer was used. Ions that were produced by bombarding the sample with 6 keV Xe atoms were accelerated through a potential of 10 kV. CAD experiments were conducted by mass selection of ions with MS-I, the mass resolution for the mass-selected ions being approximately 1000. The 10 keV mass-selected ions were then activated by collision with helium in a collision chamber floated at 8 kV. Helium gas pressure was adjusted in order to attenuate the primary ion beam by 70%. Fragment ions were detected with a JEOL ADS 11 S variable-dispersion array detector equipped with MS-II.

3-Nitrobenzyl alcohol for negative-ion MS and magic bullet (dithioerythritol/dithiothritol = 1/3) saturated with lithium hydroxide for positive-ion MS were used as matrices. All CAD spectra were obtained by using quasi-molecular anions and/or lithium-adduct cations produced by FAB as precursor ions.

Acknowledgements

The authors thank Mrs T. Chijimatsu for recording the NMR spectra.

References

Adams, J. (1990). *Mass Spectrom. Rev.*, *9*, 141.

Bouillant, M. L., Jacoud, C., Zanella, I., Favre-Bonvin, J., & Bally, R. (1994). *Phytochemistry*, *35*, 769.

Cirigottis, K. A., Cleaver, L., Corrie, J. E. T., Grasby, R. G., Green, G. H., Mock, J., Nimgirawath, S., Read, R. W., Ritchie, E., Taylor, W. C., Vadasz, A., & Webb, W. R. G. (1974). *Aust. J. Chem.*, *27*, 345.

Scannel, R. T., Barr, J. R., Murty, V. S., Reddy, K. S., & Hecht, S. M. (1988). *J. Am. Chem. Soc.*, *110*, 3650.

Su, C-J., Reusch, R. N., & Sadoff, H. L. (1981). *J. Bacteriol.*, *147*, 80.

Suzuki, Y., Esumi, Y., Hyakutake, H., Kono, Y., & Sakurai, A. (1996). *Phytochemistry*, *41*, 1485.

Suzuki, Y., Esumi, Y., Saito, T., Kishimoto, Y., Morita, T., Koshino, H., Uzawa, J., Kono, Y., & Yamaguchi, I. (1998). *Phytochemistry*, *47*, 1247.

Suzuki, Y., Esumi, Y., Uramoto, M., Kono, Y., & Sakurai, A. (1997). *Biosci. Biotech. Biochem*, *61*, 480.

Suzuki, Y., Saitoh, C., Hyakutake, H., Kono, Y., & Sakurai, A. (1996). *Biosci. Biotech. Biochem.*, *60*, 1786.

Verdeal, K., & Lorenz, K. (1977). *Cereal Chem.*, *54*, 475.